Technical Paper

Transactions of the Society of Naval Architects of Korea
Vol. 29, No.3, August 1992
大 韓 造 船 學 會 論 文 集
第 29 卷 第 3 號 1992 年 8 月

Hydrodynamic Forces and Maneuvering Characteristics of Ships at Low Advance Speed

by

Kyoung-Ho Sohn*

저속시 선체에 작용하는 조종유체력 및 조종성능에 관한 연구

손경호*

Abstract

Some practical methods have already been proposed for predicting the characteristics of ship manoeuvring motions at relatively high advance speed. However, these methods can hardly be applied to motions of ships in starting, stoppint, backing and slow steaming conditions, even though such extensive motions are of vital importance from a safety point of view particularly in harbour areas.

The method presented here aims at predicting the characteristics of ship manoeuvring at low advance speed, which covers starting, stopping, backing and slow steaming conditions. The force mathematical models at large angles of incidence to the hull as well as under the wide range of propeller operations are formulated.

Simulations of various manoeuvres at low advance speed are carried out for two types of merchant ship, i.e. a LNGC and a VLCC. Comparisons between simulations and corresponding full-scale measurements or free-running model tests provide a first verification of the proposed mathematical models.

요 약

선박이 일정속도 이상의 전진속도를 갖일 때의 조종성능 평가법은 지금까지 많이 제안되어

발 표 : 1991년도 대한조선학회 추계연구발표회('91. 11. 16.)
Manuscript received : Nov. 20, 1991, revised manuscript received : April 30, 1992.
* Member, Dept. of Naval Architecture, Korea Maritime University.

왔으나, 이들을 항만내에서의 다양한 운동모드 즉, 출발, 정지, 후진, 미속조종 등에는 적용에 무리가 있다. 본 연구에서는 출발, 정지, 후진, 미속조종 등을 포함하는 저속항행시의 조종운동 특성의 평가법을 제안하기 위해서, 대각도 횡류각 뿐만 아니라 광범위한 프로펠러 작동하에서의 선체, 프로펠러, 타에 작용하는 유체력의 특성을 수식모형화 하였다. 제안된 수식모형을 이용하여 액화가스 운반선, 대형유조선 두 선박에 대해 저속항행시의 조종운동 시뮬레이션 계산을 수행하여 실선시험 또는 모형시험 결과와 비교, 검토하였다.

1. Introduction

Recently the manoeuvring performance of ships has been of greater importance than ever from a safety point of view. This in turn has made the requirements on ship manoeuvring more demanding. There has veen international effort through the IMO(International Maritime Organization), aiming to improve ships' manoeuvrability. One current IMO activity relevant to ship manoeuvrability[1] aims to arrive at legislation for (i) Estimating manoeuvring performance at ship design stage, (ii) Full scale trials to confirm the manoeuvring performance after the ship has been built, and (iii) Issuing a more detailed manoeuvring booklet for the master and officers of the ship.

The important aspect to be considered in ship design and operation, and also to be included in the manoeuvring booklet, is the manoeuvring performance at low advance speed which covers starting, stopping backing and slow steaming conditions etc. particularly in harbour and coastal waters. In fact, ship operators require some information on manoeuvrability in which the confined operating conditions have to be considered[2].

In harbour manoeuvring, low advance speed at large drift angle becomes dominant and the effects of shallow waters and extraneous forces such as the effects of wind and current are important. Various ship motions such as accelerating, stopping, backing, slow steaming and tug operations are inevitably brought out in order to avoid collision with other ships or when approaching the wharf and vice versa. Consequently surge, sway and yaw motions have nearly the same order of magnitude, otherwise sway and yaw motions are much larger than surge motion. Under these circumstances the flows of waters around a ship become more complicated and the hydrodynamic forces on a ship are subject to the effect of the motion's history on itself, namely the fluid memory effect. Until recently, due to these difficulties we lacked the methods available for predicting harbour manoeuvring. In the background of the IMO's work, however, active research will continue to take place for the development of mathematical models suitable for harbour manoeuvring[3].

This paper presents a mathematical model for low advance speed manoeuvrability, which covers starting, stopping, backing and slow steaming conditions etc. To begin with, it is assumed at this stage that the ship is manoeuvring in deep waters and the fluid memory effect is negligible. There are three principal methods for modelling the hydrodynamic reactions on the hull. The first one is to describe the hydrodynamic reactions using polynomial expressions[4], [5], the second one is the Fourier series expansions[6], [7] and the third one is cross-flow drag expressions[8], [9]. This paper adopts the method of the Fourier series expansion for modelling the hydrodynamic reactions on the hull and uses the data of captive model tests [6] in the process of modelling. The propeller and rudder forces are also formulated in the whole region of propeller operation to cover both the ahead and astern motion. The simultaneous equations used to predict the time history of the various manoeuvres at low advance speed, are then solved by the computer for two types of merchant ship, such as a VLCC and a LNGC. The simulated manoeuvres are compared with the corresponding full-scale measurements [10], [15] or free running

odel tests [6], [10].

2. Hydrodynamic Forces on a Ship

2.1 Basic equations of manoeuvring motion

In general it is customary in manoeuvring studies to consider only the motions in the horizontal plane, namely surge, sway and yaw. To describe a ship's motion, a system of body axes(G-xyz) which are fixed on the ship and are moving relative to the space axes ($\bar{O}$-XYZ), is employed as shown in Fig. 1. The origin of body axes is located at the ship's centre of gravity G.

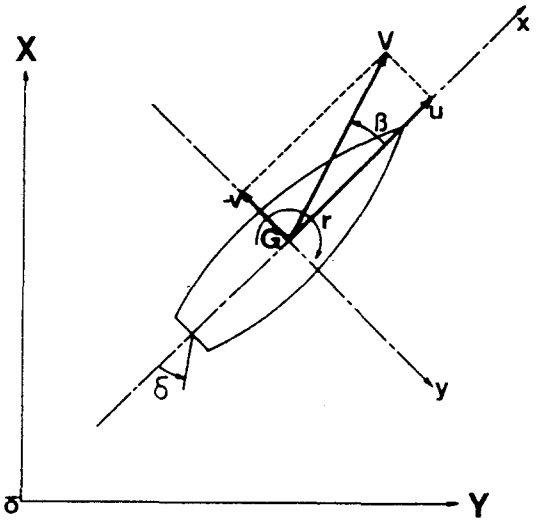

Fig. 1 Co-ordinate system

Following the sign convention of Fig. 1 and assuming that the body axes coincide with the principal axes of inertia, the equations of motion can be written as:

$$\begin{aligned} &m(\dot{u}-vr)=(\text{all the surge force})\\ &m(\dot{v}+ur)=(\text{all the sway force})\\ &I_z\dot{r}=(\text{all the yaw moment}) \end{aligned} \tag{1}$$

where m denotes the ship's mass, I_z the moment of inertia about the z axis, and a dot over the parameters of ship motion represents time derivative. According to the established procedure [11] of dealing with hydro-inertial terms involved in the right-hand side of eq.(1), this equation becomes

$$\begin{aligned} &(m+m_x)\dot{u}-(m+m_y)vr=X\\ &(m+m_y)\dot{v}+(m+m_x)ur=Y\\ &(I_z+J_z)\dot{r}=N-x_GY \end{aligned} \tag{2}$$

where X and Y denote the hydrodynamic forces (ex. hydro-inertial forces) in the x and y directions respectively, N the hydrodynamic yawing moment about the midship, x_G the distance of the centre of gravity in front of the midship, m_x and m_y denote the added mass in the x and y directions respectively, and J_z the added moment of inertia about the z axis. The added mass and added moment of inertia can be computed from potential flow theory with good accuracy. They can also be obtained from references [12], [13] and [14].

X, Y and N may generally be expressed as:

$$\begin{aligned} &X=X_H+X_P+X_R\\ &Y=Y_H+Y_P+Y_R\\ &N=N_H+N_P+N_R \end{aligned} \tag{3}$$

where the terms with subscripts H, P and R represent the damping forces on the hull, the propeller forces and the rudder forces respectively. Eq.(3) is based on the modular concept, as is the modular manoeuvring model, first developed by the Mathematical Modelling Group(MMG) of the Society of Naval Architects of Japan. The model arranged in this way lends itself to a number of applications. It allows research on one particular module and the effect that that module has on the system model as a whole.

If each of the modules in the right-hand side of eq.(3) is modelled concretely, the simultaneous differential equations (2) and (3) will then be solved by the computer to predict the time history of a manoeuvre.

2.2 Modelling of the hull damping forces

(1) In the case where a ship's speed is non-zero

Except that the ship speed V is zero, the parameters of ship motion shown in Fig. 1 and the hull damping forces are non-dimensionalised as:

$$\begin{aligned} &u', v' = u, v/V \\ &r' = rL/V \\ &X'_H\ Y'_H = X_H, Y_H/0.5\rho LdV^2 \\ &N'_H = N_H/0.5\rho L^2dV^2 \end{aligned} \tag{4}$$

where L, d and V denote length between perpendiculars, mean draft and ship speed($V=\sqrt{u^2+v^2}$) respectively, and ρ is the density of water.

The physical flow phenomena have been considered to analyse the constitution of damping forces on the bare hull with very large drift angles at low advance speed. X_H consists of hull resistance and induced drag caused by free vortices shed from the boundary layer near the hull's surface. Each of Y_H and N_H consists of three groups of forces. The first is the hydrodynamic forces generated by the irrotational flow of an otherwise undisturbed, unbounded ideal fluid in response to the ship's general motion. The second is the hydrodynamic forces generated by the ship's hull which can be considered as lifting surface in inclined flow. The third is the non-linear cross-flow forces on the hull in response to its transverse motion. Oltman [8] attempted to adopt the expressions of hull damping forces as a clear merger of ideal fluid effect, lifeing effect and cross-flow effect. The mathematical model adopted by Oltman has some advantages, which are that there are not too many hydrodynamic coefficients which have to be decided by the model tests or theoretical calculations and the model is a compact and physically motivated expression. However, it is difficult to separate the hydrodynamic forces obtained by model tests into three groups, namely ideal fluid effect, lifting effect and cross-flow effect. Furthermore, the cross-flow drag coefficients vary according to the longitudinal location of the hull. So, from a practical point of view this paper adopts the treatment in which the damping forces on the hull are expressed by the Fourier series expansion of drift angle and then the Fourier coefficients are expressed as the function of yaw angular velocity. This treatment was suggested by Takashina [6] and Yumuro [7].

Drift angle β is defined as:

$$\beta = \tan^{-1}\left(-\frac{v}{u}\right) \tag{5}$$

where β is considered to vary from zero to ± 180 degrees. Then the non-dimensional damping forces on the hull can be expressed by Fourier series expansion of β as:

$$\begin{aligned} X'_H &= X'(u') + \sum_k (S_k^X \sin k\beta + C_k^X \cos k\beta) \\ Y'_H &= \sum_k (S_k^Y \sin k\beta + C_k^Y \cos k\beta) \\ N'_H &= \sum_k (S_k^N \sin k\beta + C_k^N \cos k\beta) \end{aligned} \tag{6}$$

where $X'(u')$ denotes the ship's resistance coefficient, S_k and C_k the Fourier coefficients. S_k and C_k generally are the function of yaw angular velocity because the ship has drift angle and also yaw angular velocity as well while manoeuvring, but are constants in the pure sway motion.

The static drift test(oblique towing test) was performed by Takashina [6] with a 2.5m model of the LNG ship shown in Table 1 in order to obtain the Fourier coefficients S_k, C_k. He suggested S_1^Y, S_3^Y, S_5^Y, S_1^N, S_2^N, S_3^N and S_4^N as the terms of significance. Amongst them, the terms of S_5^Y, S_3^N and S_4^N are higher orders of very small values. So, the Fourier series expansion expressions adopted by the author are given by eq.(7) in the pure sway motion.

$$\begin{aligned} X'_H &= X'(u') + S_1^X \sin\beta \\ Y'_H &= S_1^Y \sin\beta + S_3^Y \sin 3\beta \\ N'_H &= S_1^N \sin\beta + S_2^N \sin 2\beta \end{aligned} \tag{7}$$

Fig. 2 illustrates the lateral force and yaw moment on the LNG ship model as the function of drift angle. The mark in the figure represents the measured data [6] and the curve the least square error fittings using eq.(7). The expressions

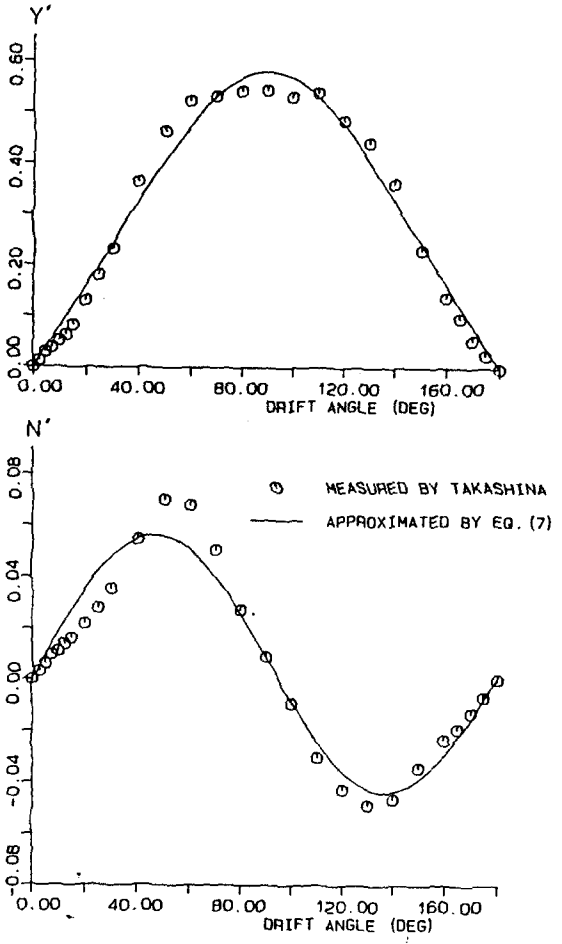

Fig. 2 Non-dimensional sway force and yaw moment on hull as a function of drift angle(2.5m model of LNGC)

in eq.(7) are much shorter and clearer than those suggested by Takashina. Furthermore, Takashina utilised a yaw rotating test where the drift angle is the funtion of yaw angular velocity, namely $\beta = rt$(t=time). He suggested S_1^Y, S_3^Y, S_5^Y, C_1^Y, C_3^Y, S_1^N, S_2^N, S_3^N, S_4^N, C_0^N, C_1^N and C_2^N by analysing the results of the test with the same model. Amongst them, the terms of C_5^Y, C_3^Y, S_3^N, S_4^N and C_1^N are higher orders of very small values. So, the Fourier series expansion expressions adopted by the author are given by eq.(8) in both the sway and yaw motions.

$$
\begin{aligned}
Y'_H &= S_1^Y \sin\beta + S_3^Y \sin 3\beta + C_1^Y \cos\beta \\
N'_H &= S_1^N \sin\beta + S_2^N \sin 2\beta \\
&\quad + C_0^N + C_2^N \cos 2\beta
\end{aligned} \tag{8}
$$

where all the Fourier coefficients are the function of yaw angular velocity. On the basis of Takashina's experimental results [6] and taking the symmetry of the ship's hull, the expressions of all the Fourier coefficients in eq.(8) are suggested by the author as:

$$
\begin{aligned}
S_1^X &= S_{11}^X r' \\
S_1^Y &= S_{10}^Y + S_{11}^Y |r'| \\
S_3^Y &= S_{30}^Y \\
C_1^Y &= C_{11}^Y r' + C_{12}^Y r' |r'| \\
S_1^N &= S_{10}^N \\
S_2^N &= S_{20}^N + S_{22}^N r'^2 \\
C_0^N &= C_{01}^N r' + C_{02}^N r' |r'| \\
C_2^N &= C_{21}^N r'
\end{aligned} \tag{9}
$$

where S_{10}^Y, S_{30}^Y, S_{10}^N and S_{20}^N coincide with S_1^Y, S_3^Y, S_1^N and S_2^N in eq.(7) respectively in case of pure sway motion. Substituting eq.(9) and the following relation:

$$
\begin{aligned}
&\sin\beta = -v' \\
&\sin 2\beta = -2u'v' \\
&\sin 3\beta = -3v' + 4v'^3 \\
&\cos\beta = u' \\
&\cos 2\beta = 1 - 2u'^2
\end{aligned} \tag{10}
$$

into eq.(8) and then expressing all the coefficients in eq.(9) in terms of the hydrodynamic derivatives widely used nowadays, the non-dimensional hull damping forces can be given as:

$$
\begin{aligned}
X'_H &= X'(u') + X'_{vr} v'r' \\
Y'_H &= Y'_v v' + Y'_{ur} u'r' + Y'_{vvv} v'^3 \\
&\quad + Y'_{vr} v'|r'| + Y'_{urr} u'r'|r'| \\
N'_H &= N'_v v' + N'_{uv} u'v' + N'_r r' \\
&\quad + N'_{vvr} v'^2 r' + N'_{uvrr} u'v'r'^2 + N'_{rr} r'|r'|
\end{aligned} \tag{11}
$$

where the relationship between the hydrodynamic

derivatives in eq.(11) and the coefficients in eq. (9) are given as:

$$\begin{aligned}
X_{vr}' &= -S_{11}^{X} \\
Y_{v}' &= -S_{10}^{Y} - 3S_{30}^{Y} \\
Y_{ur}' &= C_{11}^{Y} \\
Y_{vvv}' &= 3S_{30}^{Y} \\
Y_{vr}' &= -S_{11}^{Y} \\
Y_{urr}' &= C_{12}^{Y} \\
N_{v}' &= -S_{10}^{N} \\
N_{uv}' &= -2S_{20}^{N} \\
N_{r}' &= C_{01}^{N} + C_{21}^{N} \\
N_{vvr}' &= -2C_{21}^{N} \\
N_{uvrr}' &= -2S_{22}^{N} \\
N_{rr}' &= C_{02}^{N}
\end{aligned} \tag{12}$$

We can obtain the numerical values of the hydrodynamic derivatives in eq.(11) from appropriate model experiments. The model experiments are relatively costly and time consuming. From these points it will be useful if we can make use of the collection and parametric analysis of hydrodynamic data by Inoue [15], [16]. So, eq.(11) will be somewhat changed here without losing physical validity. The non-linear term of v', namely $Y_{vvv}' v'^3$ that appears in the second expression of eq. (11), may be replaced by the term $Y_{vv}' v'|v'|$, because $Y_{vv}' v'|v'|$ can well represent the non-linearity of v' and also the physical property of symmetry of the hull form. Furthermore, the term $N_v'v'$ in the third expression of eq.(11) represents the non-dimensional yawing moment due to the ship's transverse motion only. If the hull form of fore and aft parts is symmetrical about the midship, the numerical value of N_v' will be zero. Even a real ship may take a very small value of N_v' as revealed, for example, in the experimental result by Takashina. So, the expression of yawing moment due to transverse motion is given here by eq.(13) where the term $N_{uv}' u'v'$ is considered to include $N_v'v'$.

$$N_{uv}' u'v' = (-S_{10}^{N} - 2S_{20}^{N}) u'v' \tag{13}$$

and, for convenience, the expressions of hydrodynamic derivatives Y_{ur}', Y_{urr}', N_{uv}' and N_{uvrr}' are re-written as Y_r', Y_{rr}', N_v' and N_{vrr}' which are widely used in case of relatively high advance speed. The term $X'(u')$ in the first expression of eq.(11) is modelled by eq.(14).

$$X'(u') = X_{uu}' u'|u'| \tag{14}$$

Eventually the hull damping forces are given as:

$$\begin{aligned}
X_H &= 0.5\rho LdV^2\{X_{uu}' u'|u'| + X_{vr}' v'r'\} \\
Y_H &= 0.5\rho LdV^2\{Y_v'v' + Y_r'u'r' \\
&\quad + Y_{vv}' v'|v'| + Y_{vr}' v'|r'| + Y_{rr}' u'r'|r'|\} \\
N_H &= 0.5\rho LdV^2\{N_v'u'v' + N_r'r' \\
&\quad + N_{vvr}' v'^2r' + N_{vrr}' u'v'r'^2 + N_{rr}' r'|r'|\}
\end{aligned} \tag{15}$$

The hydrodynamic derivatives appearing in eq. (15) can be obtained from references [13], [16] and [17]. It must be pointed out that the area of application of the hydrodynamic data derived from references [13], [16] and [17] covers conventional manoeuvres at relatively high advance speed. However, we can expect that these will provide the first approximation of the hydrodynamic data necessary at low advance speed. Table 2 shows the hydrodynamic data derived from regression expressions [17] for two types of merchant ship. Here the surge hydrodynamic derivative X_{vr}' is estimated by Inoue [15] and the resistance derivative X_{uu}' by total resistance in a straight course.

(2) In the case where a ship's speed is zero

The motion, when a ship's speed V is zero, is limited to turning only with no movement at the centre of gravity of the ship. When the resultant speed of a ship is zero, the damping forces on the hull are expressed as:

$$\begin{aligned}
X_H &= 0 \\
Y_H &= 0 \\
N_H &= 0.5\rho L^4 dN_{rr}' r|r|
\end{aligned} \tag{16}$$

It must be pointed out that if the hull form is longitudinally non-symmetrical about the midship to a great extent, as for example, that of a trawler, X_H and Y_H cannot be negligible. However they can be negligible for many merchant ships.

2.3 Modelling of the propeller and rudder forces

(1) Propeller forces

The propulsion X_P under the wide range of propeller loads to cover both the ahead and astern motion is modelled as:

$$X_P=0.5\rho(1-t)[\{u(1-w_p)\}^2+(0.7\pi nD)^2] \times(\frac{\pi}{4})D^2K_T \tag{17}$$

$$K_T=\sum_{k=0}^{20}[A(k)\cos k\theta_p+B(k)\sin k\theta_p]$$
$$\theta_p=\tan^{-1}\{u(1-w_p)/(0.7\pi nD)\} \tag{18}$$

where the thrust coefficient K_T has been expressed by the Fourier series expansion [18] of hydrodynamic pitch angle θ_p, t represents thrust deduction factor, w_p propeller ake fraction, n number of propeller shaft revolutions per second, and D propeller diameter. The Fourier coefficients $A(k)$ and $B(k)$ which appear in the expression of K_T can be obtained by the propeller open-water test. They are estimated here by utilising the experimental results by Lammeren [18] with Wageningen B-Screw series, which cover the whole region of propeller operation, namely four quadrants of θ_p. The first quadrant of $\theta_p(0°\leq\theta_p\leq90°)$ is in case of $u\geq0$ and $n\geq0$, the second quadrant($90°\leq\theta_p\leq180°$) $u\geq0$ and $n\leq0$, the third quadrant($180°\leq\theta_p\leq270°$) $u\leq0$ and $n\leq0$, and the fourth quadrant($270°\leq\theta_p\leq360°$) $u\leq0$ and $n\geq0$. On the other hand, as the expressions of eqs.(17) and (18) cover a wide range of propeller load, the values of thrust calculated by the expression lack some accuracy in the first quadrant where the most accurate values are required. For this reason only in the first quadrant, namely in the case of $u\geq0$ and $n\geq0$, the propulsion X_P is given according to reference [19] as:

$$X_P=\rho n^2D^4\{C_1-C_2(\frac{u}{nD})\} \tag{19}$$

$$C_1=(\frac{C_T}{2s_o})(\frac{S_A}{Ld})(\frac{L}{D})(\frac{d}{D})J_{so}^2$$
$$C_2=C_1(1-w_{po})\frac{D}{P} \tag{20}$$

where C_T represents total resistance coefficient in a straight course, s slip ratio which will be defined in eq.(28), P propeller pitch, S_A wetted surface area of the hull, and J_s apparent advance coefficient($J_s=u/nD$), the expression with subscript o in s, J_s and w_p like s_o, J_{so} and w_{po} represents the values of s, J_s and w_p in a straight course. Generally the thrust deduction factor t and propeller wake fraction w_p are treated as functions of ship motion and propeller operating condition. Here t is assumed constant and w_p is given by:

$$w_p=w_{po}\exp\{-4.0(\beta-x_p'r')^2\} \tag{21}$$

where x_p' is the x coordinate of propeller location non-dimensionalised by ship length L. w_{po} and t are estimated here by Takashiro's method [20]. The expressions $w_{po}=0$ and $t=0$, nevertheless, are adopted regardless of eq.(21) in case of $u\leq0$.

The propeller induced sway force and yaw moment are expressed as:

$$Y_P=\rho n^2D^4Y_p^*$$
$$N_P=\rho n^2D^4LN_p^* \tag{22}$$

where the coefficients Y_p^* and N_p^* are considered in the second quadrant only, namely $u\geq0$ and $n\leq0$, and obtained from the experimental result by Fujino [21] as the function of the apparent advance coefficient which is defined as:

$$J_p=\frac{u}{nP} \tag{23}$$

(2) Rudder forces

The rudder forces are expressed as:

$$X_R=-c_{RX}F_N\sin\delta$$

$$Y_R=-(1+a_H)\ F_N\cos\delta$$
$$N_R=-(x_R+a_H x_H)\ F_N\cos\delta \tag{24}$$

where δ represents the rudder angle, F_N the normal force produced by the rudder, and x_R the x coordinate of rudder location. The coefficients c_{RX}, a_H and x_H are correction factors to adapt the open-water characteristics of rudder to behind-hull conditions. The values of them are estimated from reference [22] as the function of the block coefficient. The normal force produced by the rudder F_N is expressed according to Fujii [23] as:

$$F_N=\frac{1}{2}\rho A_R V_R^2\ \frac{6.13\lambda}{\lambda+2.25}\ \sin\alpha_R \tag{25}$$

where λ and A_R are the rudder's aspect ratio and its submerged area respectively, V_R the effective in-flow velocity over the rudder, and α_R the effective angle of attack. The following expressions are employed for V_R and α_R.

$$V_R=\sqrt{u_R^2+v_R^2}$$
$$\alpha_R=\delta+\delta_0-\gamma(\beta-l_R' r') \tag{26}$$

$$\delta_0=\frac{\pi s_o}{90} \tag{27}$$

$$\gamma=C_p\ C_s$$
$$C_p=\frac{1}{\sqrt{1+0.6\eta(2-1.4s)s/(1-s)^2}}$$
$$C_s=0.45|\beta-l_R' r'|\ ;\quad |\beta-l_R' r'|\leq 1.111$$
$$C_s=0.5\ ;\quad |\beta-l_R' r'|>1.111$$
$$s=1-u(1-w_p)/nP$$
$$\eta=\frac{D}{H} \tag{28}$$

where u_R and v_R represent the longitudinal and lateral components of the effective in-flow velocity to rudder respectively, δ_0 the offset rudder angle necessary for straight forward running, γ the flow straightening(rectification) coefficient due to both the ship's hull and propeller, H rudder height, and l_R' experimental coefficient the value of which is taken as $l_R'=-0.9$ from reference [22]. The u_R and v_R in eq.(26) are expressed according to Yoshimura [24] as:

$$u_R=\varepsilon nP\sqrt{1-2(1-\eta k)s+\{1-\eta k(2-k)\}s^2}$$
$$v_R=u_R\tan\{\gamma(\beta-l_R' r')\} \tag{29}$$

$$\varepsilon=(1-w_R)/(1-w_p)$$
$$k=0.6/e$$
$$w_R=w_p w_{Ro}/w_{po} \tag{30}$$

where w_{Ro} represents the wake fraction at the rudder location in straight forward running, the value of which is generally taken as $w_{Ro}=0.45$ for models and $w_{Ro}=0.25$ for fullscales [15], [24]. The expressions $u_R=0$ and $v_R=0$, nevertheless, are adopted regardless of eq.(29) in case of $u\leq 0$, and the expression $u_R=u(1-w_p)$ is adopted in place of the first expression of eq.(29) in case of both $u>0$ and $s<0$ or in case of $n=0$.

(3) Movements of propeller and rudder

The number of propeller shaft revolutions is assumed to respond to the ordered one through the main engine telegraph as:

$$\dot{n}=(n^*-n)/T_n \tag{31}$$

where n^* is the ordered one through the main engine telegraph, and T_n the time constant of main engine. The value of T_n is taken here as $T_n=15$ sec for a full-scale ship.

The mathematical model for the dynamics of electro-hydraulic steering gear is given by eq. (32).

$$\dot{\delta}=(\delta^*-\delta)/T_E\ ;\ |\delta^*-\delta|\leq T_E|\dot{\delta}_{max}|$$
$$\dot{\delta}=\mathrm{sign}(\delta^*-\delta)|\dot{\delta}_{max}|\ ;\ |\delta^*-\delta|>T_E|\dot{\delta}_{max}| \tag{32}$$

where δ^* is the ordered rudder angle, T_E the time constant of the steering gear, and $\dot{\delta}_{max}$ maximum rudder speed. The values of T_E and $|\dot{\delta}_{max}|$ are taken here as $T_E=2.5$ sec and $|\dot{\delta}_{max}|$

=3.0 deg/sec for a full-scale ship.

3. Simulation of Manoeuvering Characteristics

The simulation calculation has been carried out on the basis of the mathematical model described in section 2 with hydrodynamic data shown in Table 2 for two types of merchant ship, VLCC and LNGC. The calculated results are compared with the published full-scale measurements [10], [15] for VLCC and free-running model tests [6], [10] for LNGC. However, all the simulation calculations have been carried out for full-scale ships, both VLCC and LNGC.

Table 1 Principal particulars of ships

Item		VLCC	LNGC
HULL			
Length B. P.	L(m)	318.00	270.00
Breadth	B(m)	56.00	44.82
Mean draft	d(m)	20.58	10.80
Trim	(m)	0.0	0.0
Block coefficient	C_B	0.827	0.692
RUDDER			
Area ratio	A_R/Ld	1/58.6	1/44.5
Aspect ratio	λ	1.55	1.25
PROPELLER			
Diameter	D(m)	8.90	8.0
Pitch ratio	P/D	0.71	0.8
No. of blades		5	4

Table 2 Hydrodynamic derivatives and coefficients

	VLCC	LNGC
m_x/m	0.120	0.075
m_y/m	0.839	0.721
J_z/mL^2	0.044	0.042
X'_{uu}	−0.00826	−0.00957
X'_{vr}	−0.09775	−0.06630
Y'_v	−0.40720	−0.28648
Y'_r	0.10166	0.06283
Y'_{vv}	−0.33312	−0.40217
Y'_{vr}	−0.33129	−0.31193
Y'_{rr}	−0.02965	−0.03461
N'_v	−0.12943	−0.080
N'_r	−0.05314	−0.0368
N'_{vvr}	−0.13380	−0.06686
N'_{vrr}	0.07094	0.01004
N'_{rr}	−0.01206	−0.02470
t	0.24	0.20
w_{po}	0.458	0.26
w_{Ro}	0.25	0.25
c_{RX}	0.81	0.76
a_H	0.63	0.38
x'_H	−0.46	−0.46

The mathematical model adopted here has been worked out for manoeuvring motions mainly at low advance speed. Even so, it has been intended to apply the mathematical model to conventional turning manoeuvres at relatively high advance speed. Figs. 3, 4 and 5 show comparisons between the simulated and measured paths for conventional turning characteristics. Fig. 3 shows a comparison for a 35 degree rudder to starboard turn with an initial speed of 16.5 knots of VLCC. Figs. 4 and 5 show comparisons for a 15 degree rudder to port turn and a 35 degree rudder to port turn respectively, with an initial speed of 20.0 knots of LNGC.

Fig. 6 compares the simulated and measured paths for the accelerating turn of the LNGC. The accelerating turn has been performed here by ordering not only the number of propeller shaft revolutions necessary for the speed of 20 knots in a straight course but also the 35 degree rudder to port from a stationary condition. Fig. 7 compares

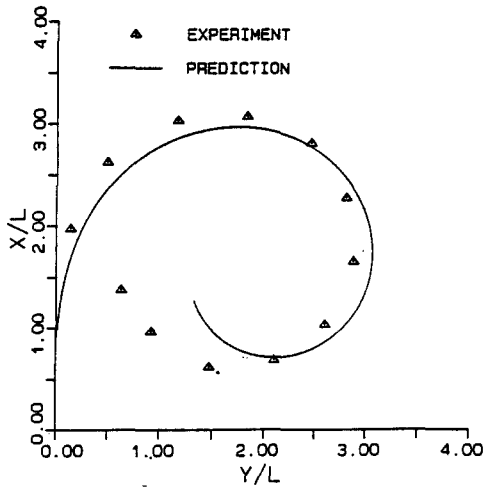

Fig. 3 Conventional turn of VLCC (rudder angle=35deg.)

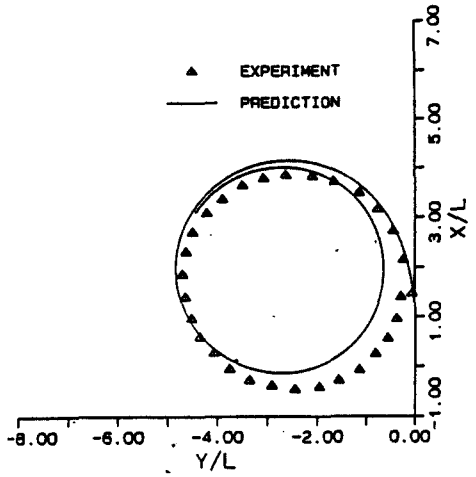

Fig. 4 Conventional turn of LNGC (rudder angle=−15deg.)

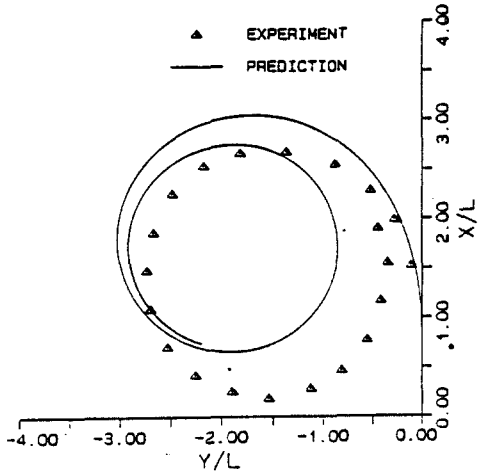

Fig. 5 Conventional turn of LNGC (rudder angle=−35deg.)

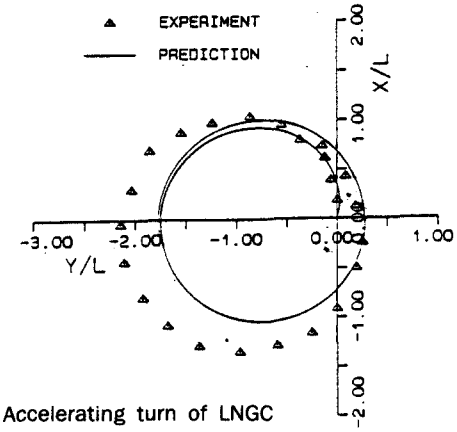

Fig. 6 Accelerating turn of LNGC (rudder angle=−35deg.)

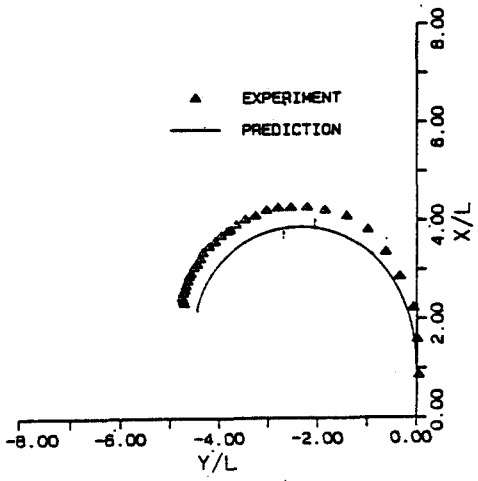

Fig. 7 Coasting turn of LNGC (rudder angle=−35deg.)

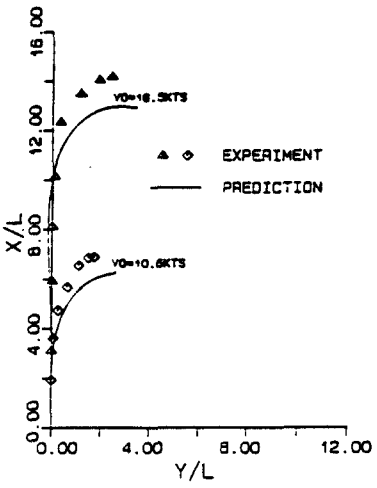

Fig. 8 Stopping distance of VLCC

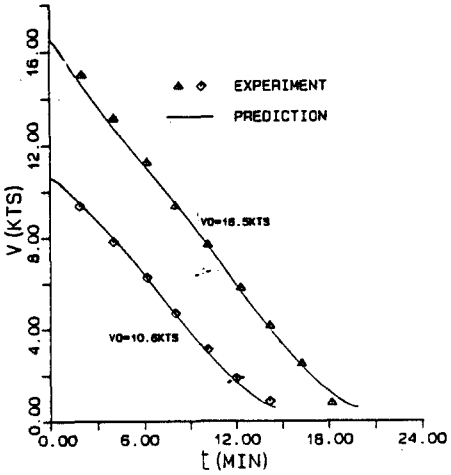

Fig. 9 Stopping time of VLCC

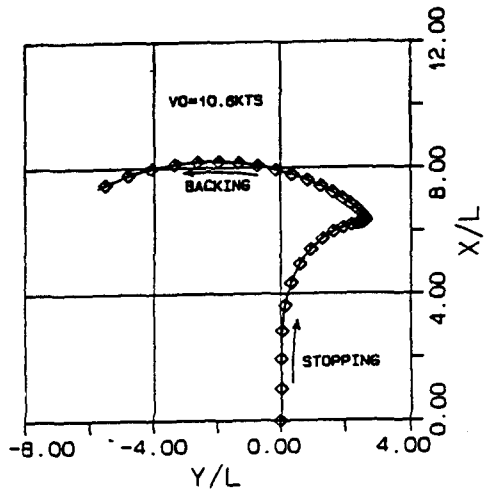

Fig. 10 Stopping and backing motion trajectories of VLCC

the simulated and measured paths for the coasting turn of LNGC. The coasting turn has been performed here by ordering not only the number of propeller shaft revolutions to zero but also the 35 degree rudder to port from the steady straight running condition of 20 knots forward speed. Figs. 8 and 9 show comparisons for stopping distances and stopping times of VLCC respectively. The symbol V_o in Figs. 8 and 9 represents the initial ship speed in the steady straight motion. The stopping motion has been made here by ordering the number of revolutions of the propeller shaft to "full astern" from "full ahead" and "half ahead", the speeds of which are 26.5 knots and 10.6 knots respectively. The number of "full astern" revolutions of the propeller shaft corresponds to −70% of that of "full ahead" in a steady straight course. Fig. 10 illustrates the simulated path during stopping and backing motion of the VLCC, which has been made by ordering the number of revolutions of the propeller shaft to "full astern" from "half ahead".

The above comparisons show, to some extent, satisfactory correlations between computer simulations and full-scale or model experiments for the various manoeuvres at low advance speed. Furthermore, it is noted that the proposed mathematical model is useful for the prediction of conventional manoeuvres at relatively high advance speed.

4. Conclusion

The mathematical model and computer simulation for prediction of manoeuvring characteristics mainly at low advance speed are discussed. Hydrodynamic damping forces acting on the hull at low advance speed and at very large angles of incidence are expressed by the Fourier series expansion and then in terms of hydrodynamic derivatives. Propeller forces and rudder forces are modelled in the whole region of propeller opeation. All the input data required for solving the proposed mathematical model can be obtained from published experimental data or from parametric expressions of hydrodynamic forces for practical purposes.

The computer simulation has been carried out for two types of merchant ship on the basis of the proposed mathematical model. Comparison between the computer predictions and full-scale measurements or model experiments demonstrate satisfactory agreement. The proposed mathematical model will be utilised for the evaluation of ship manoeuvrability not only at low advance speed but also at relatively high advance speed at the preliminary ship design stage.

The prediction method of this work may extensively be applied to other areas such as port design, sefety study of traffic systems in harbour areas and towing operations by tug boats.

References

[1] IMO, "Interim Guidelines for Estimating Manoeuvring Performance in Ship Design", MSC/Circ. 389, 10 January 1985.

[2] Coates, G.A., A Ship-Handler's View, *Proceedings of the International Conference on Ship Manoeuvrability*, Vol.1, London, RINA, 1987.

[3] Fujino, M., et al., MMS Report I-IV, *Bulletin of the Society of Naval Architects of Japan*, No.717−721, 1989(in Japanese).

[4] Kobayashi, E. et al., A Simulation Study on Ship Manoeuvrability at Low Speeds, *Proceedings of the International Conference on Ship Manoeuvrability*, Vol.1., London, RINA, 1987.

[5] Kose, K. et al., "On a Mathematical Model of Manoeuvring Motions of Ships in Low Speeds, *Journal of the Society of Naval Architects of Japan*, Vol.155, 1984(in Japanese).

[6] Takashina, J., "Ship Manoeuvring Motion due to Tug Boats and its Mathematical Model", *Naval Architecture and Ocean Engineering, Japan, Vol.25*, 1987.

[7] Yumuro, A., "Some Experiments on Manoeuvring Hydrodynaic Forces in Low Speed Condition, *Journal of the Kansai Society of Naval Architects, Japan*, No.209, 1988(in Japanese).

[8] Oltmann, P. et al., "Simulation of Combined Engine and Rudder Manoeuvres Using an Improved Model of Hull-Propeller-Rudder Interaction, *15th Symposium on Naval Hydrodynamics*, 1984.

[9] Yoshimura, Y., "Mathematical Model for the Manoeuvring Ship Motion in Shallow Water (2nd Report)-Mathematical Model at Low Forward Speed-, *Journal of the Kansai Society of Naval Architects*, Japan, No.210, 1988(in Japanese).

[10] Hirano, M. et al., "A Practical Method of ship Manoeuvring Motion and Its Application", *Proceedings of the International Conference on Ship Manoeuvrability*, Vol.Ⅱ, London, RINA, 1987.

[11] Newman, J.N., "Marine Hydrodynamics", MIT Press, pp.135-140, 1978.

[12] Motora, S., "On the Measurement of Added Mass and Added Moment of Inertia for Ship Motions(Part 1, 2 and 3), *Journal of the Society of Naval Architects of Japan*, Vol.105, 106, 1959, 1960(in Japanese).

[13] Clarke, D. et al., "The Application of Manoeuvring Criteria in Hull Design Using Linear Theory", *The Naval Architect*, RINA, 1983.

[14] Hooft, J.P. et al., "Manoeuvrability of Frigates in Waves", *Marine Technology*, Vol.25, No.4, 1988.

[15] Inoue, S. et al., "A Practical Calculation Method of Ship Manoeuvring Motion, *International Shipbuilding Progress*, Vol.28, No.325, 1981.

[16] Inoue, S. et al., Hydrodynamic Derivatives on Ship Manoeuvring, *International Shipbuilding Progress*, Vol.28, No.320, 1981.

[17] Hooft, J.P. et al., "Design Information on the Ship Manoeuvrability", *NSMB Report*, No.4 5931-1/2-NS, 1984.

[18] Lammeren, W.P.A. et al., "The Wageningen B-Screw Series", *Trans. of SNAME*, Vol.77, 1969.

[19] Sohn, K.H., On the Mathematical Model for Estimating Manoeuvring Performance of Ships, *Journal of the Korean Institute of Navigation*, Vol.13, No.2, 1989(in Korean).

[20] Takashiro, K., Power Prediction Based on Modified Yamagate Resistance Chart and Newly Introduced Thrust Deduction and Wake Factor, *Journal of the Kansai Society of Naval Architects*, Japan, No.177, 1980.

[21] Fujino, M. et al., On the Manoeuvrability of Ships while Stopping by Adverse Rotation of Propeller(2nd Report), *Journal of the Kansai Society of Naval Architects, Japan, No.173, 1979(in Japanese)*.

[22] Kose, K. et al., Mathematical Model and Model Experiment for Estimating Manoeuvrability, *Bulletin of the Society of Naval Architects of Japan*, No.668, 1985(in Japanese).

[23] Fujii, J., Experimental Research on Rudder Performance(1st Report), *Journal of the Society of Naval Architects of Japan*, Vol.107, 1960(in Japanese).

[24] Yoshimura, Y. et al., Modelling of Manoeuvring Behaviour of Ships with a Propeller Idling, Boosting and Reversing, *Journal of the Society of Naval Architects of Japan*, Vol.144, 1978 (in Japanese).